Self-Assembly of Amphiphilic Nanoparticle−Coil "Tadpole" Macromolecules

Jae Youn Lee and Anna C. Balazs*

Department of Chemical and Petroleum Engineering, University of Pittsburgh, Pittsburgh, Pennsylvania 15261

Russell B. Thompson

Theoretical Division, Los Alamos National Laboratory, Los Alamos, New Mexico 87545

Randall M. Hill

Dow Corning Corporation, Midland, Michigan 48686-0994

Received October 13, 2003
Revised Manuscript Received April 2, 2004

Introduction. There has been considerable fascination with the self-assembling behavior of amphiphilic chainlike molecules that range from short-chain surfactants to high molecular weight block copolymers. The self-assembly of simple amphiphiles into membranes may have played an important role in the origin of life.[1] The self-organization of amphiphiles with more complex architectures can lead to a stunning variety of complex morphologies.[2,3] In the case of short-chain surfactants, the equilibrium morphology of the self-assembled system depends on geometric factors, such as the ratio of the "head" to "tail" sizes.[4] Here, the headgroups are small molecules and the tails are coillike. In the case of block copolymers, the structure of the melt depends on the relative composition of the chains, the degree of polymerization, and the incompatibility between the different blocks.

It is intriguing to think of another potentially self-assembling system, one in which the tail is still a coillike molecule but the attached "head" is a nanoparticle. In this scenario, the coil and the surface of the headgroup are incompatible, and this incompatibility could drive the organization of these "tadpole" molecules into spatially periodic, nanoscale structures. Recent theoretical[5] and experimental studies[6−9] involving mixtures of nanoscopic inorganic particles and diblock copolymers have focused on harnessing the microphase separation of the copolymers to template the self-assembly of nanoparticles and, in this manner, create nanostructured organic/inorganic hybrid materials. The use of amphiphilic organic/inorganic tadpoles, where the heads are formed from inorganic particles and the tails are synthetic polymers, could provide an alternative route for creating such ordered nanocomposites. As we show below, the single-tailed tadpoles also display distinct interfacial activity when blended with diblock copolymers. If the heads were covered with multiple, uniformly distributed hairs, the species would preferentially localize in the hair-compatible phase. However, with a single hair, the tadpole behaves like a surfactant, with a head localized in one phase and the tail in the other. These interfacial interactions can be exploited to control the spatial distribution of the tadpoles within a copolymer melt, yielding an additional means of designing novel nanocomposites.

One challenge to investigating the properties of these tadpoles is synthesizing the macromolecules so that the nanoparticle head is coated with just a single hair. Promising experiments are currently underway to anchor a single chain onto gold nanoparticles.[10] Another challenge is developing a theoretical approach for predicting the equilibrium structure of the system. In previous studies,[5] we developed a model that integrates a self-consistent-field theory (SCFT) and a density functional theory (DFT) to investigate the phase behavior of mixtures of nanoparticles and diblock copolymers. Experimental studies[6] have recently confirmed our "SCF/DFT" predictions on the entropically driven size segregation of binary particle mixtures within a diblock melt.[11,12] Experiments[7] have also validated our observation that added nanoparticles can promote transitions between the different structures of the diblock copolymers.[13]

In this paper, we extend this SCF/DFT model to examine the equilibrium structure of a melt of novel amphiphilic "copolymers", where each copolymer consists of a linear flexible chain that is anchored to the surface of a solid, spherical particle. In this SCF/DFT approach, the SCFT captures the thermodynamic behavior of the anchored chain, and the DFT describes the ordering and steric interactions of the particle. Using this method, we examine the behavior of AB tadpoles, which have an A tail and an incompatible B head. We find that the phase behavior of these hybrid molecules differs significantly from that of pure AB diblocks with the same effective composition. We also derive an expression to describe the self-assembly of ABC tadpoles where the anchored chain is an AB diblock and C is an incompatible particle. We specifically focus on the case where C is chemically identical to the B species and find that the ABB molecules organize in a way that is distinct from the AB tadpoles. Finally, we highlight one example of a mixture of AB diblocks and tadpoles to illustrate a method for tailoring the structure of organic/inorganic nanocomposites.

The Model. A volume V is filled with n tadpole molecules, where each molecule consists of an A-like linear, flexible chain that is attached to a B-like spherical, hard particle of radius R. To further characterize this system, we define a set of variables that are specific to the tadpole architecture. We define N/ρ_0 to be the volume of the tadpole, where N is the degree of polymerization of a fictive, linear chain whose segment volume is ρ_0^{-1}. The variable f is the volume fraction of the A-like chain in the molecule. In terms of these definitions, the total volume of each molecule is $v_t = v_A + v_R = N/\rho_0$, where the volume of the linear chain moiety is $v_A = fN/\rho_0$ and the volume of the sphere moiety is $v_R = (1 - f)N/\rho_0 = 4\pi R^3/3$. For a given volume v_t, f and R are not independent, and we specify R and determine f according to the relation $f = 1 - (v_R/v_t)$. In addition, we describe the incompatibility between A and B species with the Flory−Huggins parameter χ, which characterizes the interaction between A monomers that are in contact with the B particles. Thus, the system is characterized by the following three independent variables: R (or f), N, and χ. Finally, we assume that the system is incompressible.

10.1021/ma035542q CCC: $27.50
Published on Web 04/20/2004

The following concentration operators describe the distribution of each species:

$$\hat{\varphi}_A(\mathbf{r}) = \frac{N}{\rho_0}\sum_\alpha \int_0^f ds\ \delta(\mathbf{r} - \mathbf{r}_\alpha(s)) \quad (1)$$

$$\hat{\varphi}_B(\mathbf{r}) = \frac{1-f}{v_R}\int_{|\mathbf{r}'|<R} d\mathbf{r}'\ \hat{\rho}_B(\mathbf{r}' + \mathbf{r}) \quad (2)$$

$$\hat{\rho}_B(\mathbf{r}) = \frac{N}{\rho_0}\sum_{\alpha=1}^{n} \delta(\mathbf{r} - \mathbf{r}_\alpha(f) - R\hat{\mathbf{n}}_\alpha) \quad (3)$$

where the subscripts A and B denote the A-like coil and B-like sphere, respectively, and $\hat{\rho}_B$ is the distribution operator for the centers of the spheres. The $\mathbf{r}_\alpha(s)$ describe the space curve occupied by the A chains in the αth tadpole. A unit vector $\hat{\mathbf{n}}_\alpha$ is introduced in (3) to indicate the direction between the end of the coil, which is attached to the surface of the sphere, and the center of the sphere of the αth tadpole. The unit vector for this tadpole is

$$\hat{\mathbf{n}}_\alpha = \sin\theta_\alpha \cos\phi_\alpha \hat{\mathbf{i}} + \sin\theta_\alpha \sin\phi_\alpha \hat{\mathbf{j}} + \cos\theta_\alpha \hat{\mathbf{k}} \quad (4)$$

where $\hat{\mathbf{i}}$, $\hat{\mathbf{j}}$, and $\hat{\mathbf{k}}$ are the three Cartesian unit vectors. The angles θ_α and ϕ_α are measured from the respective z and x axes in the conventional way for spherical coordinates.

Following the procedure in refs 14−16, the partition function for the system of tadpoles subject to the fields W_i can be written using functions instead of operators as

$$Z = \int \mathscr{D}\Phi_A \mathscr{D}\rho_B \mathscr{D}W_A \mathscr{D}W_B \mathscr{D}\Xi Q^n \exp\left\{-\frac{\rho_0}{N}\int d\mathbf{r}\ [\chi N \Phi_A \Phi_B - W_A\Phi_A - W_B\rho_B - \Xi(1 - \Phi_A - \Phi_B)]\right\} \quad (5)$$

where the functions Φ_i and ρ_B replace the corresponding concentration operators and the partition function for a single tadpole Q is given by

$$Q \equiv \int d\hat{\mathbf{n}}_\alpha \int \mathscr{D}\mathbf{r}_\alpha P[\mathbf{r}_\alpha;0,f] \exp\{-\int_0^f ds\ W_A(\mathbf{r}_\alpha(s)) - W_B(\mathbf{r}_\alpha(f) + R\hat{\mathbf{n}}_\alpha)\} \quad (6)$$

We assume that the tails are Gaussian chains so the weighting factor for individual configurations is given by

$$P[\mathbf{r}_\alpha; s_1, s_2] = \exp\left\{-\frac{3}{2Na^2}\int_{s_1}^{s_2} ds \left|\frac{d}{ds}\mathbf{r}_\alpha(s)\right|^2\right\} \quad (7)$$

in analogy with the properties of the coils in the case of rod−coil diblocks.[15] Here, a is the statistical segment length.

From the mean-field approximation of (5), we obtain a free energy expression for the system; we add a correction term to this expression to account for the steric interactions between the hard-sphere heads. This approach follows reasoning described previously[17] and gives a free energy of

$$\frac{NF}{\rho_0 k_B T V} = -\ln\left(\frac{QfN}{V\rho_0}\right) + \frac{1}{V}\int d\mathbf{r}\ [\chi N \varphi_A(\mathbf{r})\,\varphi_B(\mathbf{r}) - w_A(\mathbf{r})\,\varphi_A(\mathbf{r}) - w_B(\mathbf{r})\,\rho_B(\mathbf{r}) - \xi(1 - \varphi_A(\mathbf{r}) - \varphi_B(\mathbf{r})) + \rho_B(\mathbf{r})\Psi(\bar{\varphi}_B(\mathbf{r}))] \quad (8)$$

where Ψ is the Carnahan−Starling free energy per particle,[18] $\bar{\varphi}_B(\mathbf{r})$ is a "smoothed" sphere density obtained from the Tarazona DFT,[19] k_B is Boltzmann's constant, and T is the temperature. The respective fields $w_i(\mathbf{r})$ and the local volume fractions $\varphi_i(\mathbf{r})$ are functions for which the free energy attains its minimum. We vary the free energy with respect to each of the independent functions to obtain the mean-field equations,[14−16,20] which allow us to solve the system self-consistently. As a result, we obtain the densities and fields for various possible morphologies, with the lowest free energy phase being the equilibrium state.

This model can be easily extended to describe an ABC copolymer in which an AB diblock is attached to a C type sphere. As before, we specify the radius R and determine the fraction of the diblock portion f. An additional parameter f_A, the fraction of the A sites within the diblock, is needed to complete the description of the system. The total volume of the molecule is then $v_t = v_A + v_B + v_R$, where $v_A = f_A f N/\rho_0$, $v_B = (1 - f_A)fN/\rho_0$, and $v_R = 4\pi R^3/3 = (1 - f)N/\rho_0$. The distribution operators of each species are defined similarly to (1)−(3), and the free energy is written as

$$\frac{NF}{\rho_0 k_B T V} = -\ln\left(\frac{QfN}{V\rho_0}\right) + \frac{1}{V}\int d\mathbf{r}\ [\chi_{AB} N \varphi_A(\mathbf{r})\,\varphi_B(\mathbf{r}) + \chi_{AC} N \varphi_A(\mathbf{r})\,\varphi_C(\mathbf{r}) + \chi_{BC} N \varphi_B(\mathbf{r})\,\varphi_C(\mathbf{r}) - w_A(\mathbf{r})\,\varphi_A(\mathbf{r}) - w_B(\mathbf{r})\,\varphi_B(\mathbf{r}) - w_C(\mathbf{r})\,\rho_C(\mathbf{r}) - \xi(1 - \varphi_A(\mathbf{r}) - \varphi_B(\mathbf{r}) - \varphi_C(\mathbf{r})) + \rho_C(\mathbf{r})\Psi(\bar{\varphi}_C(\mathbf{r}))] \quad (9)$$

where additional terms are introduced to reflect the additional interactions between the different species.

To obtain solutions to the mean-field equations, we implement the combinatorial screening technique of Drolet and Fredrickson.[21] In addition, we minimize our free energy with respect to the size of the simulation box.[22]

Results and Discussion. In this short communication, there is only room to describe illustrative examples that capture the unique behavior of these tadpoles; we will explore the phase space in more detail in future studies. Here, we first examine the morphology of a melt of AB tadpoles and then compare this morphology to the one found for ABB systems, where each molecule consists of an AB diblock tail and a B head.

The volume of an AB tadpole is set equal to the volume of a linear chain whose invariant polymerization index $\bar{N} = N\rho_0^2 a^6 = 1000$, where a is the statistical segment length. The sphere radius is set to $R = 0.15R_0$, where $R_0 = aN^{1/2}$ is the root-mean-square end-to-end distance of the $\bar{N} = 1000$ chain. Here, we set $a = 1$. We then calculate f as $(\rho_0/N)(N/\rho_0 - 4\pi R^3/3) = (1 - (4\pi/3)(0.15)^3\bar{N}^{1/2})$, which yields $f = 0.55$. Thus, this system corresponds to 55% coil and 45% sphere. The incompatibility parameter is set to $\chi N = 30$; at such a large value, we anticipate that system will undergo microphase separation.

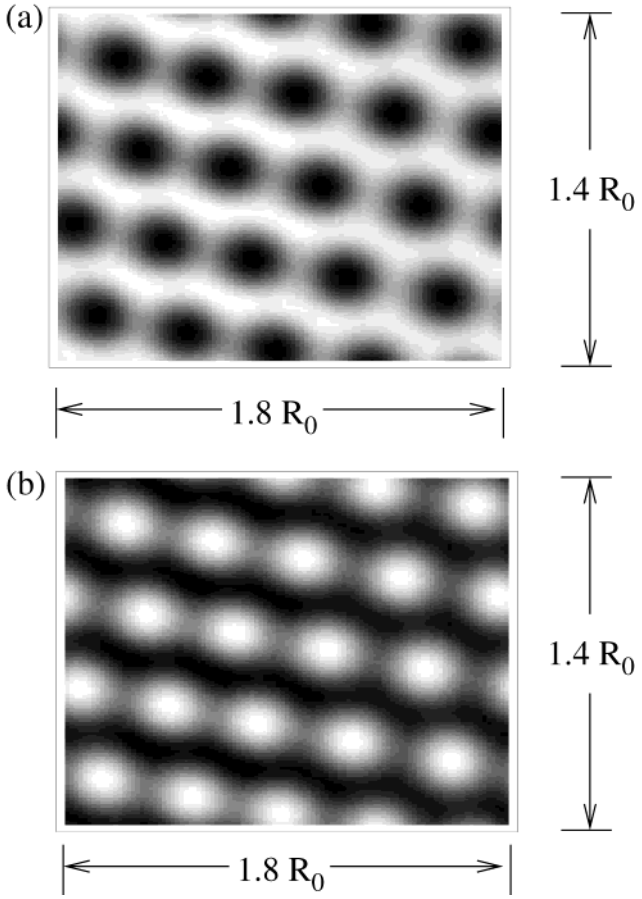

Figure 1. Two-dimensional plots for the tadpole system. Plots are for $\chi N = 30$, $f = 0.55$, and $R = 0.15R_0$. The plot in (a) represents the distribution of the A tails, and the plot in (b) represents the distribution of the B heads. Light regions indicate a high density, while dark regions indicate low densities. The images show that the system displays a close-packed hexagonal structure.

Figure 1 shows a two-dimensional density contour plot for the coil and sphere portions in the tadpole system. The material clearly displays a hexagonal close-packed morphology; the same structure is also observed in the three-dimensional calculations. This finding is relatively surprising since for a 55/45 A/B composition, a pure diblock melt would exhibit a lamellar morphology. Thus, it appears that the tadpoles self-organize in a manner that is distinct from these diblock chains. This observation agrees with recent findings from Brownian dynamics simulations on nanoparticles functionalized with oligomeric tethers.[23]

In Figure 2, we plot the one-dimensional density profiles for the AB tadpoles and the 55/45 AB diblocks. These profiles are not projections of 2D density profiles along a certain axis. Rather, the density distributions are obtained by assuming translational invariance along two spatial axes. Although this assumption fails to capture the correct morphology of the pure tadpole system, these 1D plots help in further pinpointing differences in the equilibrium structures for the two cases. The plots reveal that there is a greater degree of overlap between the A and B fragments in the tadpoles than in the diblocks. The stretched chains can more readily segregate from each other than the spherical head and tail. Another obvious difference between the two systems is that the period of the AB domains is much smaller for the tadpoles than the diblocks; this

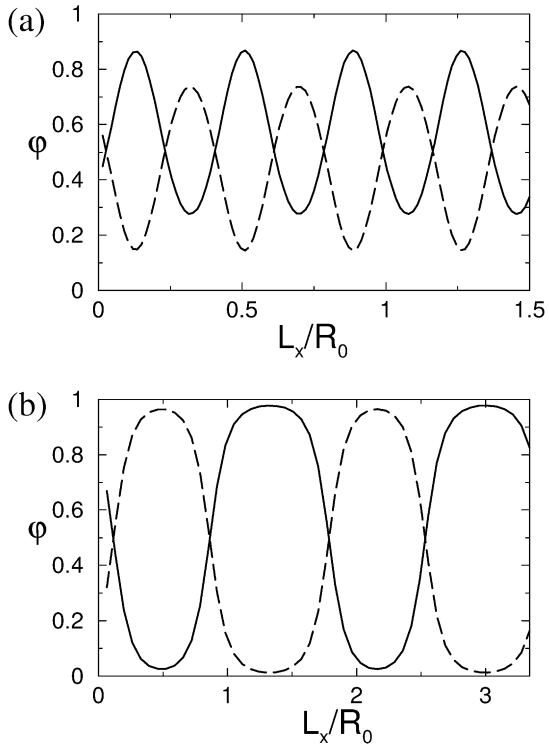

Figure 2. One-dimensional density profiles for (a) the 55/45 tadpole melt and (b) a 55/45 AB diblock melt. For the tadpoles, the parameters are identical to those used in Figure 1. For the diblock, $\bar{N} = 1000$ and $\chi N = 30$. Solid curves represent the distribution of the A-like species, and the dashed lines mark the distribution of the B-like species.

behavior can be attributed to the steric interactions between the solid spheres. Because of packing constraints, the solid headgroups are less effective than chains at associating into large domains; hence, the period is smaller in the tadpole system. If B-like chains where present in the tadpole melt, these chains could fill the void space between the hard sphere, and the system could, as we will show in the next example, form a lamellar structure. Here, however, there are no B chains to fill the voids, and the system cannot assemble into a lamellar morphology but must take on a hexagonal structure.

A close look at the distribution of headgroups in Figure 1 seems to indicate that each sphere-rich region corresponds to a single sphere of radius $R = 0.15R_0$. With respect to this unusual feature, it is interesting to contrast the self-assembling behavior of the tadpoles with the micellization of surfactant molecules with a bulky headgroup. In the case of such surfactants in solution, the head-to-tail ratio determines the micellar structure.[4] In the case of a melt of tadpoles with solid heads, steric interactions between the spheres dominate the behavior of the system, resulting in a possible formation of "unimolecular micelles".

To diminish the effect of the steric repulsion between the spheres, we attach an AB diblock chain to a sphere. Here, the B block is anchored to surface of the B-like particle. Figure 3 reveals the density profiles for a melt of such molecules, where $\chi N = 30$, $R = 0.1R_0$, and $f_A = 0.6$. The parameters were selected so that the overall AB composition corresponds to one yielding a lamellar morphology. Here, the A-like coil portion is approximately 52% of the total volume, while the B-like coil and the sphere portions make up the rest. Unlike the

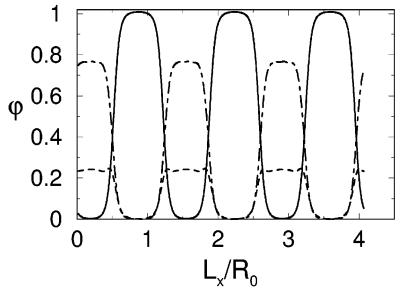

Figure 3. One-dimensional density profiles for ABB tadpole systems. The parameters are $\chi N = 30$, $R = 0.1R_0$, and $f_A = 0.6$. The A-like coil portion is approximately 52% of the total volume, while the B-like coil and the sphere portions make up 48%. The solid curve represents the distribution of the A block, and the dot−dashed curve represents the distribution of the B block in the AB tail; the dashed curve marks the distribution of the solid B heads.

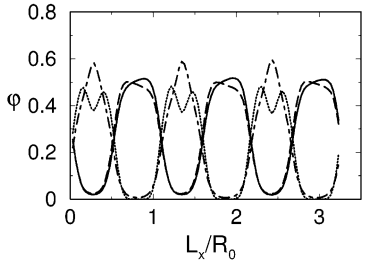

Figure 4. One-dimensional density profiles for the 50/50 mixture of 55/45 tadpoles and diblocks shown in Figure 2. The solid curve represents the distribution of the A monomers of the diblock, while the dot−dashed curve marks the B monomers of the diblock. The distribution of the A tail of the tadpole is represented by the long-dashed curve, and the distribution of the solid B head is marked by the dotted curve.

AB tadpole case, the ABB tadpoles can aggregate to form a lamellar structure, as shown in Figure 3 and confirmed by 2D calculations on this system. As noted above, the B-like chains can fill the void sites between the hard-sphere heads. This behavior is clearly visible in Figure 3, where the dot−dashed black lines mark the location of the B blocks and show that these blocks extend throughout the B particle domains. As a consequence, the B domains can form stripes and the entire system can exhibit a lamellar phase.

In the final example, we consider a 50/50 mixture of the 55/45 AB diblocks and 55/45 tadpoles. The calculation involves adding the SCFT terms for the pure diblocks[14,17] to the expression in (8). This mixture also forms a lamellar structure, and Figure 4 shows the 1D density plots for the system. By comparing this plot with Figure 2a, we can see that the presence of the diblocks leads to sharper, narrower interfaces between the A and B domains. Note that the spheres now essentially form a bilayer within the B domains.

Conclusions. In summary, we have developed a numerical model for describing the phase behavior of tadpole copolymers, which are formed by attaching a flexible chain to a solid, nanoscopic headgroup. Using this approach, we have shown that the phase behavior of tadpole copolymers can differ significantly from that of compositionally comparable diblocks. This difference in behavior is due to the presence of steric interactions between the hard spheres in the tadpole system. These findings can be exploited to create nanostructured composite materials that exhibit specific geometries and properties. For example, a linear polymer can be anchored to a solid nanoparticle with a specific, desired index of refraction, and the resulting spatially periodic system can display novel optical properties. If the particles exhibit unique electromagnetic behavior, the closely spaced particles in the resultant material can yield optimal electrical or magnetic properties.

As the studies on the ABB system indicated, the arrangement of the nanoparticles can be tailored by anchoring block copolymers onto the surface of the nanoparticles. The addition of AB diblocks to the melt of tadpoles also provides a means of controlling the overall morphology of the system and the distribution of particles within the material. Further studies are currently underway to examine the phase behavior of mixtures of diblock copolymers and AB or ABC tadpole molecules. These studies will provide additional guidelines for creating nanostructured materials with controlled morphologies.

Acknowledgment. The authors acknowledge helpful discussions with Prof. Mark Matsen. Financial support from Dow-Corning Corp. is gratefully acknowledged.

References and Notes

(1) Monnard, P. A.; Deamer, D. W. *Anat. Rec.* **2002**, *268*, 196.
(2) Wei, Z.; Wang, Z.-G. *Macromolecules* **1995**, *28*, 7215.
(3) Li, W.; Gersappe, G. *Macromolecules* **2001**, *34*, 6783 and references therein.
(4) Israelachvili, J. N. *Intermolecular and Surface Forces*; Academic Press: London, 1985.
(5) Balazs A. C. *Curr. Opin. Solid State Mater. Sci.* **2003**, *7*, 27 and references therein.
(6) Bockstaller, M. R.; Lapetnikov, Y.; Margel, S.; Thomas, E. L. *J. Am. Chem. Soc.* **2003**, *125*, 5276.
(7) Yeh, S.-W.; Wei, K.-H.; Sun, Y.-S.; Jeng, U.-S.; Liang, K. S. *Macromolecules* **2003**, *36*, 7903.
(8) (a) Lauter-Pasyuk, V.; et al. *Langmuir* **2003**, *19*, 7783. (b) Lauter-Pasyuk, V.; Lauter, H. J.; Ausserre, D.; Gallot, Y.; Cabuil, V.; Hamdoun, B.; Kornilov, E. I. *Physica B* **1998**, *248*, 243.
(9) Lopes, W. A.; Jaeger, H. M. *Nature (London)* **2001**, *414*, 735 and references therein.
(10) Huo, Q. Polymer and Coatings Department, North Dakota State University, private communication.
(11) Thompson, R. B.; Lee, J. Y.; Jasnow, D.; Balazs, A. C. *Phys. Rev. E* **2002**, *66*, 031801.
(12) Lee, J. Y.; Thompson, R. B.; Jasnow, D.; Balazs, A. C. *Phys. Rev. Lett.* **2002**, *89*, 155503.
(13) Lee, J. Y.; Thompson, R. B.; Jasnow, D.; Balazs, A. C. *Macromolecules* **2002**, *35*, 4855.
(14) Matsen, M. W.; Schick, M. *Phys. Rev. Lett.* **1994**, *72*, 2660.
(15) Matsen, M. W.; Barrett, C. *J. Chem. Phys.* **1998**, *109*, 4108.
(16) Matsen, M. W. *J. Phys.: Condens. Matter* **2002**, *14*, R21.
(17) Thompson, R. B.; Ginzburg, V. V.; Matsen, M. W.; Balazs, A. C. *Macromolecules* **2002**, *35*, 1060.
(18) Carnahan, N. F.; Starling, K. E. *J. Chem. Phys.* **1969**, *51*, 635.
(19) Tarazona, P. *Mol. Phys.* **1984**, *52*, 81.
(20) In solving the mean-field equations, it is necessary to solve a modified diffusion equation, which is detailed elsewhere.[16] The propagators $q(\mathbf{r},s)$ and $q^{\dagger}(\mathbf{r},s)$ which appear in the diffusion equation must have the initial conditions $q(\mathbf{r},0) = 1$ and $q^{\dagger}(\mathbf{r},f) = \int d\hat{\mathbf{n}} \exp\{-w_B(\mathbf{r} + R\hat{\mathbf{n}})\}$. The first condition is standard, but the second is unique to this architecture.
(21) Drolet, F.; Fredrickson, G. H. *Phys. Rev. Lett.* **1999**, *83*, 4317.
(22) Bohbot-Raviv, Y.; Wang, Z.-G. *Phys. Rev. Lett.* **2000**, *85*, 3428.
(23) Zheng, Z.; Horsch, M. A.; Lamm, M. H.; Glotzer, S. C. *Nano Lett.* **2003**, *3*, 1341.

MA035542Q